Circuits and Systems, **2014, 5, 27-37**
Published Online January 2014 (http://www.scirp.org/journal/cs)
http://dx.doi.org/10.4236/cs.2014.51005

Scientific Research

Anti-Windup Digital Control Design for Time-Delayed Analog Nonlinear Systems Using Approximated Scalar Sign Function

Warsame H. Ali[1*], Yongpeng Zhang[2], Jian Zhang[1], John H. Fuller[1], Leang-San Shieh[3]
[1]Electrical & Computer Engineering Department, Prairie View A & M University, Prairie View, USA
[2]Engineering Technology Department, Prairie View A & M University, Prairie View, USA
[3]Electrical & Computer Engineering Department, University of Houston, Houston, USA
Email: [*]whali@pvamu.edu, ypzhang@pvamu.edu, lshieh@uh.edu

Received November 4, 2013; revised December 4, 2013; accepted December 11, 2013

ABSTRACT

This paper describes an approximated-scalar-sign-function-based anti-windup digital control design for analog nonlinear systems subject to input constraints. As input saturation occurs, the non-smooth saturation constraint is modeled with the approximated scalar sign function which is a smooth nonlinear function. The resulting nonlinear model is further linearized at any operating point with the optimal linearization technique, and Linear Quadratic Regulator (LQR) is then applied for a state-feedback controller optimal for each operating point. As input saturation is encountered, an iterative procedure is developed to adjust control gains by systematically updating LQR weighting matrices until the inputs lie within the saturation limits. Through global digital redesign, the analog LQR controller is converted to an equivalent digital one for keeping the essential control performance, and moreover, delay compensation is taken into account during digital redesign for compensating the potential time delays in a control loop. The swing-up and stabilization control of single rotary inverted pendulum system is used to illustrate and verify the proposed method.

KEYWORDS

Anti-Windup Control; Scalar Sign Function; Sampled-Data System; Time-Delayed System

1. Introduction

Various types of hardware limitations always exist in practical control systems with potential effects on the final control performance. A typical one encountered in practice is actuator saturation. For instance, as common actuation devices, motors have limited speed and torque range, power sources have output bounds, control valves cannot be more than fully open or fully closed, etc. As the control command is saturated at the top or bottom limit during actuator saturation, the control loop is broken and the controller loses the ability to regulate plant's behavior for the time being. This phenomenon, called controller windup, may lead to significant degradation in control performance, such as long settling time, high overshoot or even instability [1].

In order to circumvent the windup effect, there exist many anti-windup approaches in the literature in the past decades. Most of them are proposed for linear systems, like the extensively-studied two-phase approach [1-4] (a nominal linear controller is first designed with the saturation constraints ignored and then a conditioning scheme is developed for reducing the windup effects of saturation) and Linear Matrix Inequalities (LMI)-based methods [5-7]. To the authors' knowledge, however, few anti-windup approaches have been developed for nonlinear systems. The very limited efforts include the work of converting the physical constraint problem to a state-dependent constraint problem through a coordinate transformation method [8,9], and those based on input-output linearization or feedback linearization [8-11].

[*]Corresponding author.

This paper proposes an approximated-scalar-sign-function-based anti-windup technique for analog nonlinear systems with input constraints. As a non-differentiable function, sign function or absolute-value function has the inherent capability to describe the instantaneous jumps where the system model loses smoothness, so they commonly appear in many analytical models of non-smooth nonlinearities, such as Bouc-Wen hysteresis model [12,13] and Stribeck friction model [14]. In this paper, sign function is used to represent the constrained input functions, capturing the instantaneous behavior as saturation occurs. In order to solve the non-differentiability due to sign function, approximated scalar sign function in [15] is utilized. Arising from the matrix sign function and the matrix sector function [15,16], the approximated scalar sign function is able to approximate the sign function in a smooth rational form with adjustable accuracy. Compared with other approximation techniques, like Hyperbolic tangent function, the approximated scalar sign function is stable in numerical evaluation. The constrained input functions represented with the approximated scalar sign function are differentiable, then optimal linearization in [17] is applied for the local linear model at any operating point and a state-feedback controller is developed via Linear Quadratic Regulator (LQR) for each point. As saturation occurs, an iterative procedure is developed to systematically adjust control gains by tuning the LQR weighting matrices until the saturation limits are not violated.

In addition to input constraints, time-delayed systems are another practical concern in the proposed design. This concern arises from the fact that in a sampled-data control system which is a popular control scheme nowadays due to the advance of computer technology, some fundamental operations like controller computation, A/D and D/A conversions, sensing and actuation etc, could cause time delays in the control loop. Another example is networked control systems where components communicate with each other through a real-time network, which inevitably causes transmission delays. Ignoring the delays in a control loop may lead to the failure of designed control so it is of practical interest to extend the developed anti-windup methodology to time-delayed systems. In this paper, the authors propose an input-delay-compensating digital redesign approach: an analog state-feedback controller is first designed in the delay-free case for the desired control performance; then a digital controller is obtained from the analog one through global digital redesign with the delay compensation considered. The resulting digital controller is able to maintain the essential control performance of the analog counterpart even in a time-delayed environment.

The rest of this paper is organized as follows. Section 2 introduces preliminary techniques used in the proposed anti-windup design, including approximated scalar sign function, optimal linearization and LQR. In Section 3, a global digital redesign method is developed for input delay compensation. The proposed anti-windup methodology is described in Section 4. Section 5 gives simulation results of proposed method on the swing up and stability control of single rotary inverted pendulum. Finally, the paper is concluded in Section 6.

2. Preliminaries

A) Approximated Scalar Sign Function

The scalar sign function is defined in [18] as

$$sign(z)=\begin{cases}1 & \text{if } \mathrm{Re}(z)>0\\ -1 & \text{if } \mathrm{Re}(z)<0\end{cases} \tag{1}$$

where $z\in \mathrm{C}^-\bigcup \mathrm{C}^+$, C^- and C^+ denotes the open left-half complex plane and the open right-half complex plane, respectively. It is noted that the imaginary axis $\mathrm{Re}(z)=0$ is undefined in $sign(z)$.

The scalar sign function has an alternative form in [15] as

$$sign(z)=z/\sqrt{z^2} \tag{2}$$

where $z\in \mathrm{C}^-\bigcup \mathrm{C}^+$ and

$$\sqrt{z^2}=\begin{cases}z & \text{if } \mathrm{Re}(z)>0\\ -z & \text{if } \mathrm{Re}(z)<0\end{cases} \tag{3}$$

It is also reported in [15] that $\sqrt{z^2}$, called the principal square-root of z^2, can be expanded into a continued fraction form as

$$\sqrt{z^2}=1+\cfrac{z^2-1}{2+\cfrac{z^2-1}{2+\cdots}} \tag{4}$$

and its j-th truncation can be written as

$$\left(\sqrt{z^2}\right)_j=z\frac{(1+z)^j+(1-z)^j}{(1+z)^j-(1-z)^j},\ \text{for } j=1,2,\cdots \tag{5}$$

It can be shown that the j-th truncation (5) gives the better approximation of (3) as the value of j approaches the infinity, *i.e.*

$$\lim_{j\to\infty}\left(\sqrt{z^2}\right)_j=\sqrt{z^2}=\begin{cases}z & \text{if } \mathrm{Re}(z)>0\\ -z & \text{if } \mathrm{Re}(z)<0\end{cases} \tag{6}$$

Replacing $\sqrt{z^2}$ in (2) with the j-th truncation (5) yields the approximated scalar sign function for a complex number $z\in \mathrm{C}^-\bigcup \mathrm{C}^+$ as

$$sign_j(z)=\frac{(1+z)^j-(1-z)^j}{(1+z)^j+(1-z)^j} \tag{7}$$

where $j\in \mathrm{Z}^+$ which denotes the positive integer set. It

can be inferred from (6) that (7) has the limit

$$\lim_{j\to\infty} sign_j(z) = sign(z) = \begin{cases} 1 & \text{if } \mathrm{Re}(z) > 0 \\ -1 & \text{if } \mathrm{Re}(z) < 0 \end{cases} \tag{8}$$

Particularly, the approximated scalar sign function for a real number $\sigma \neq 0$ is

$$sign_j(\sigma) = \frac{(1+\sigma)^j - (1-\sigma)^j}{(1+\sigma)^j + (1-\sigma)^j}, \quad \text{for } j \in \mathrm{Z}^+ \tag{9}$$

which has the limit

$$\lim_{j\to\infty} sign_j(\sigma) = sign(\sigma) = \begin{cases} 1 & \text{if } \sigma > 0 \\ -1 & \text{if } \sigma < 0 \end{cases} \tag{10}$$

If the definition of scalar sign function for real numbers is extended to include zero, *i.e.*

$$sign(\sigma) = \begin{cases} 1 & \text{if } \sigma > 0 \\ 0 & \text{if } \sigma = 0 \\ -1 & \text{if } \sigma < 0 \end{cases} \tag{11}$$

then

$$\lim_{j\to\infty} sign_j(\sigma) = sign(\sigma) \quad \text{for } \sigma \in \mathrm{R}, \tag{12}$$

as $sign_j(0) = 0$.

The concern of this paper is limited to the real number case (9) and the definition (11) is considered. Differentiating the approximated scalar sign function (9) with respect to the real number σ yields

$$\frac{\mathrm{d}\left(sign_j(\sigma)\right)}{\mathrm{d}\sigma} = \frac{2j\left[(1-\sigma)^{j-1}(1+\sigma)^j + (1+\sigma)^{j-1}(1-\sigma)^j\right]}{\left[(1+\sigma)^j + (1-\sigma)^j\right]^2} \tag{13}$$

for $\sigma \in \mathrm{R}$. It is easy to find that (13) is continuous everywhere, which proves the approximated scalar sign function (9) is differentiable everywhere.

Figure 1(a) gives a big scope of the evaluated approximated scalar sign function (9) for different values of *j*, and **Figure 1(b)** shows the figure detail near zero. The corresponding derivative (13) is shown in **Figure 2(a)** and the figure detail near zero in **Figure 2(b)**. It can be found from **Figure 1** that the larger the value of *j* is, the closer the curve of the approximated scalar sign function (9) approaches the one of the scalar sign function (11), so *j* is also called the approximation order in the following context. **Figure 2** shows that the approximated scalar sign function (9) is differentiable everywhere because its derivative value is always finite with the largest one located at $\sigma = 0$, equal to the approximation order *j*.

By utilizing the approximated scalar sign function, an approximate model can be obtained for a non-smooth

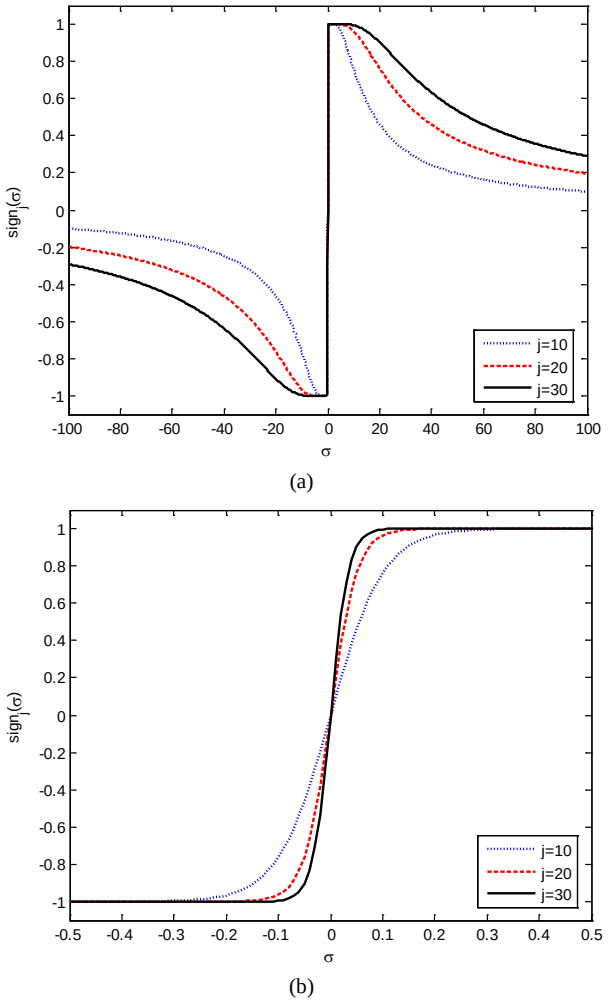

Figure 1. Approximated scalar sign function.

dynamical system with sign function constraints, whose approximation accuracy can be adjusted with the approximation order *j*. Due to the smoothness and nonlinearity of the approximated scalar sign function, the resulting approximate model is still nonlinear, but differentiable everywhere, which makes possible the further local linearization.

Remark 1: As shown in **Figure 1**, $|sign_j(\sigma)| \leq 1$ for *j* is even. This property will be exploited in the proposed anti-windup method in Section IV.

B) Optimal Linearization

Local linearization is a typical way of handling nonlinear systems and the most popular technique is Jacobian linearization [19]. However, as pointed out in [17,20], Jacobian Linearization usually produces an affine rather than linear model even at the equilibrium operating point. The only exception case is that the operating point is an equilibrium at the origin, which cannot be ensured throughout a nonlinear control process.

In order to circumvent the limitation of Jacobian linearization, Teixeira and Zak formulated linearization prob-

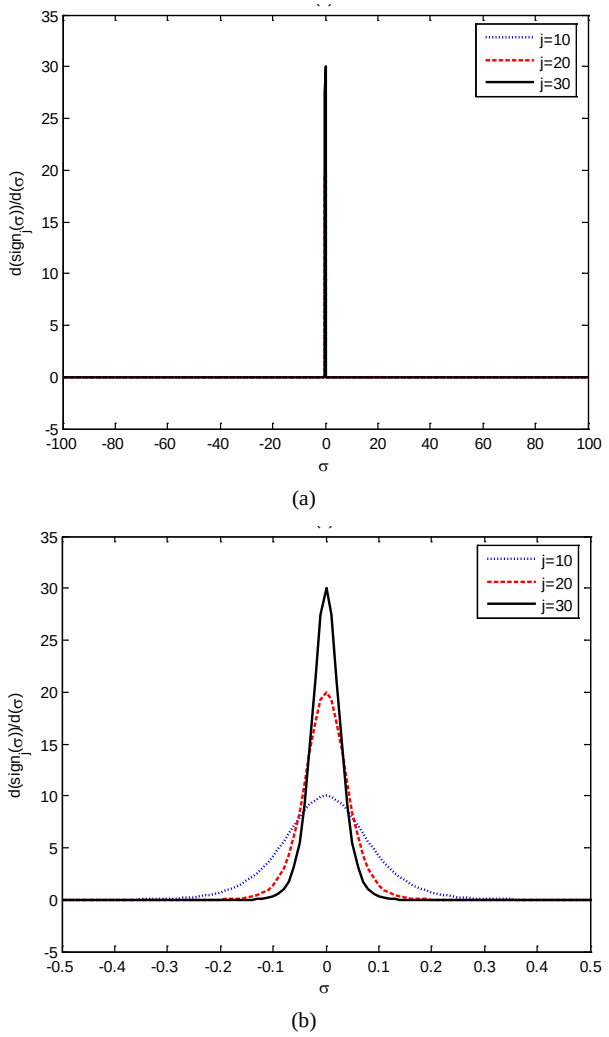

Figure 2. Derivative of approximated scalar sign function.

lem as a convex constrained optimization problem and proposed an optimal linearization approach in [17]. According to this approach, an optimal local linear model can be achieved at any operating point, which possesses the exact dynamics of the original nonlinear system at the operating point and minimum approximation error (in the least square sense) in the neighborhood of that point. Due to the space limit, only the final conclusions are briefed below.

Consider a general class of nonlinear system in the form

$$\dot{x}(t) = f\left(x(t)\right) + G\left(x(t)\right)u(t) \tag{14}$$

where $x(t) \in \Re^n$ is the state vector, $u(t) \in \Re^m$ is the input vector, $f(\cdot): \Re \to \Re^n$ with $f(0) = 0$ is a differentiable nonlinear function vector and $G(\cdot): \Re^m \to \Re^n$ is a function matrix. Its optimal local linear model at an arbitrary operating point x_k is in the state-space form

$$\dot{x}(t) = A_k x(t) + B_k u(t) \tag{15}$$

where

$$A_k = \begin{cases} \nabla f\left(x_k\right) + \dfrac{f\left(x_k\right) - \nabla f\left(x_k\right)x_k}{\left\|x_k\right\|_2^2} x_k^{\mathrm{T}} & \text{for } x_k \neq 0 \\ \nabla f(0) & \text{for } x_k = 0 \end{cases} \tag{16}$$

$$B_k = G\left(x_k\right) \tag{17}$$

$\nabla f\left(x_k\right)$ is the Jacobian matrix of $f(x)$ evaluated at the operating point x_k. It is noted that the case for $x_k = 0$ in (16) agrees with the aforementioned exception case of the operating point being an equilibrium at the origin.

Remark 2: When $f(x)$ in (14) is a scalar nonlinear function, (16) is reduced to a scalar number as

$$A_k = \begin{cases} f\left(x_k\right)/x_k & \text{for } x_k \neq 0 \\ f'(0) & \text{for } x_k = 0 \end{cases}.$$

C) Analog Linear Quadratic Regulator

Together with a linear output equation, the linearized state Equation (15) constitutes a complete local linear model as

$$\dot{x}(t) = A_k x(t) + B_k u(t) \tag{18a}$$

$$y(t) = Cx(t) \tag{18b}$$

where $y(t) \in \Re^p$ is the controlled output vector and $C \in \Re^{p \times n}$ is a constant matrix. According to LQR [21], if the linear system (18) is both controllable and observable, the optimal control law to minimize the performance index

$$J = \int_0^\infty \left\{ \left[Cx(t) - r(t)\right]^{\mathrm{T}} Q \left[Cx(t) - r(t)\right] + u^{\mathrm{T}}(t) R u(t) \right\} \mathrm{d}t \tag{19}$$

with $Q \geq 0$ and $R > 0$, is then given by

$$u(t) = -K_{ck} x(t) + E_{ck} r(t) \tag{20}$$

where

$$K_{ck} = R^{-1} B_k^{\mathrm{T}} P_k \tag{21}$$

$$E_{ck} = -R^{-1} B_k^{\mathrm{T}} \left[\left(A_k - B_k K_{ck}\right)^{-1} \right]^{\mathrm{T}} C^{\mathrm{T}} Q \tag{22}$$

$r(t)$ is the reference for the controlled output $y(t)$ to track, and P_k is the positive definite and symmetric solution of the Ricatti equation

$$A_k^{\mathrm{T}} P_k + P_k A_k - P_k B_k R^{-1} B_k^{\mathrm{T}} P_k + C^{\mathrm{T}} Q C = 0 \tag{23}$$

The weighting matrices Q and R should be tuned to make the resulting analog controller (20) give a desired control performance in the delay-free case.

3. Digital Redesign with Delay Compensation

For time-delayed systems where delays can be caused by

network transmission, controller computation, A/D and D/A conversions etc, a delay compensating technique is proposed next based on global digital redesign. Compared with the conventional digital redesign methods that the conversion is limited in the scope of the controller, like the bilinear transformation $s = 2(z-1)/[T(z+1)]$ [22], closed-loop global digital redesign techniques take into account the closed-loop nature of the whole control system, so the resulting digital controller is able to maintain the essential performance of the analog counterpart even with a low sampling frequency [20,23-25].

For a Single-Input-Single-Output (SISO) plant, the time delays in a control loop from network transmission, controller computation, A/D and D/A conversions, sensing and actuation etc, can be combined and then allocated to either the input or the output side of the plant for control design purpose [26]. The input side is used in this paper, so the local linear model (15) is modified to include the time delays as

$$\dot{x}(t) = A_k x(t) + B_k u(t-\tau) \tag{24}$$

where τ is the combined input delay. Among global digital redesign methods, the prediction-based digital redesign in [20] reduces the conversion errors by shifting the digital control signal to defined inter-sampling instant, which is readily extendable for input delay compensation. This method is briefly introduced as follows and then extended to develop the proposed digital controller featuring the input delay compensation.

The analog linear plant (18) and the analog control law (20) constitute a complete analog control system as depicted in **Figure 3(a)** where the subscript c is intended to differ from the following equivalent hybrid system which is subscripted with *d*. Suppose the equivalent hybrid system as depicted in **Figure 3(b)** and formulated by

$$\dot{x}_d(t) = A_k x_d(t) + B_k u_d(t) \tag{25a}$$

$$y_d(t) = C x_d(t) \tag{25b}$$

$$u_d(kT) = -K_{dk} x_d(kT) + E_{dk} \bar{r}(kT) \tag{25c}$$

where the analog control input $u_d(t)$ is a piecewise-constant signal generated from the digital control input $u_d(kT)$ through Zero Order Hold (ZOH) as $u_d(t) = u_d(kT)$ for $kT \le t \le (k+1)T$, and the digital state $x_d(kT)$ is the sample of the analog state $x_d(t)$ at the sampling instant $t = kT$; T is the sampling/control period. Equation (25c) is the digital control law to be designed so that the closed-loop state $x_d(t)$ in the hybrid system can closely match the closed-loop state $x_c(t)$ in the analog system at defined inter-sampling instant.

The solution $x_c(t)$ of (18a) at $t = t_v = kT + vT$ for $0 \le v \le 1$ is

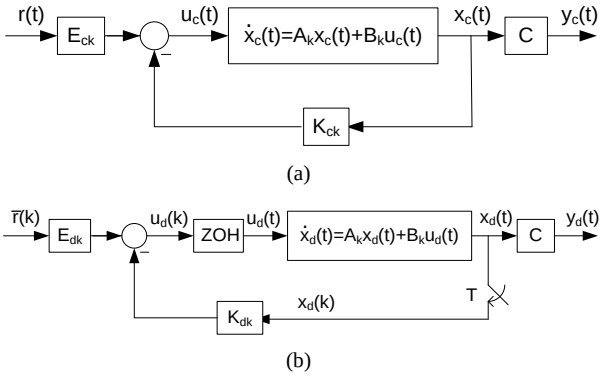

Figure 3. Analog control system and its equivelent hybrid cotnrol system.

$$\begin{aligned} x_c(t_v) &\approx \exp(A_k vT)\, x_c(kT) \\ &\quad + \int_{kT}^{kT+vT} \exp[A_k(kT+vT-\lambda)] B_k \mathrm{d}\lambda u_c(t_v) \\ &= G_k^{(v)} x_c(kT) + H_k^{(v)} u_c(t_v) \end{aligned} \tag{26}$$

where $u_c(t_v)$ is a piecewise-constant input,

$$G_k^{(v)} = \exp(A_k vT)$$

and

$$\begin{aligned} H_k^{(v)} &= \int_{kT}^{kT+vT} \exp[A_k(kT+vT-\lambda)] B_k \mathrm{d}\lambda \\ &= (G_k^{(v)} - I_n) A_k^{-1} B_k \end{aligned},$$

in which I_n is an identity matrix of appropriate dimension. The solution $x_d(t)$ of (25a) at $t = t_v$ is

$$\begin{aligned} x_d(t_v) &= \exp(A_k vT)\, x_d(kT) \\ &\quad + \int_{kT}^{kT+vT} \exp[A_k(kT+vT-\lambda)] B_k \mathrm{d}\lambda u_d(kT) \\ &= G_k^{(v)} x_d(kT) + H_k^{(v)} u_d(kT) \end{aligned} \tag{27}$$

Comparing (27) with (26) yields that with the assumption of $x_d(kT) = x_c(kT)$, the condition of $x_d(t_v) = x_c(t_v)$ is $u_d(kT) = u_c(t_v)$, which leads to the prediction-based digital controller

$$\begin{aligned} u_d(kT) = u_c(t_v) &= -K_{ck} x_c(t_v) + E_{ck} r(t_v) \\ &= -K_{ck} x_d(t_v) + E_{ck} r(t_v) \end{aligned} \tag{28}$$

By substituting (27) into (28), $u_d(kT)$ is solved as

$$u_d(kT) = (I_m + K_{ck} H_k^{(v)})^{-1} [-K_{ck} G_k^{(v)} x_d(kT) + E_{ck} r(t_v)] \tag{29}$$

where I_m is an identity matrix of appropriate dimension. As a result, the desired digital control law (25c) is found from (29) having digital control gains

$$K_{dk} = (I_m + K_{ck} H_k^{(v)})^{-1} K_{ck} G_k^{(v)} \tag{30a}$$

$$E_{dk} = (I_m + K_{ck} H_k^{(v)})^{-1} E_{ck} \tag{30b}$$

and the digital reference $\bar{r}(kT) = r(kT + vT)$. The parameter v can be tuned to adjust the control performance.

Next, the conclusion in (28) will be extended for the input delay compensation. Considering the combined input delay τ, the state equation (25a) in the hybrid system is changed to

$$\dot{x}_d(t) = A_k x_d(t) + B_k u_d(t-\tau) \tag{31}$$

In order to compensate the input delay, the digital control input $u_d(kT)$ in (28) should be further predicted for the delay duration τ as

$$u_d(kT) = u_c(t_v + \tau) = -K_{ck} x_d(t_v + \tau) + E_{ck} r(t_v + \tau) \tag{32}$$

where the future state $x_d(t_v + \tau)$ needs to be predicted based on the available signals $x_d(kT)$ and $u_d(kT)$.

Compared with the sampling/control period, the time delays from controller computation, A/D and D/A conversions etc, are relatively small, so a reasonable assumption is made in the following reasoning for simplicity purpose that the total duration of time delays in the control loop should not be larger than a sampling period, *i.e.* the combined input delay $\tau \le T$. As for the case that $\tau > T$, the proposed method can still handle but will produce a more complicated controller structure.

Let $\sigma = \dfrac{\tau}{T}$, so $0 \le \sigma \le 1$ and $\tau = \sigma T$. The solution $x_d(t)$ of (31) at $t = t_v + \tau$ is

$$\begin{aligned} x_d(t_v + \tau) &= x_d\left[kT + (v+\sigma)T\right] \\ &= G_k^{(v+\sigma)} x_d(kT) + H_{1k}^{(v+\sigma)} u_d\left[(k-1)T\right] \\ &\quad + H_{0k}^{(v+\sigma)} u_d(kT) \end{aligned} \tag{33}$$

where

$$G_k^{(v+\sigma)} = \exp\left[A_k (v+\sigma)T\right], \quad H_{0k}^{(v+\sigma)} = \left(G_k^{(v)} - I_n\right) A_k^{-1} B_k$$

and $H_{1k}^{(v+\sigma)} = \left(G_k^{(v+\sigma)} - G_k^{(v)}\right) A_k^{-1} B_k$.

By substituting (33) into (32), $u_d(kT)$ is solved as

$$\begin{aligned} u_d(kT) = \left(I_m + K_{ck} H_{0k}^{(v+\sigma)}\right)^{-1} \Big\{ & -K_{ck} G_k^{(v+\sigma)} x_d(kT) \\ & -K_{ck} H_{1k}^{(v+\sigma)} u_d\left[(k-1)T\right] + E_{ck} r(t_v + \tau) \Big\} \end{aligned} \tag{34}$$

As a result, the desired digital controller for input delay compensation is derived from (34) as

$$u_d(kT) = -K_{dk} x_d(kT) - D_{dk} u_d\left[(k-1)T\right] + E_{dk} \bar{r}(kT) \tag{35}$$

where

$$K_{dk} = \left(I_m + K_{ck} H_{0k}^{(v+\sigma)}\right)^{-1} K_{ck} G_k^{(v+\sigma)} \tag{36a}$$

$$D_{dk} = \left(I_m + K_{ck} H_{0k}^{(v+\sigma)}\right)^{-1} K_{ck} H_{1k}^{(v+\sigma)} \tag{36b}$$

$$E_{dk} = \left(I_m + K_{ck} H_{0k}^{(v+\sigma)}\right)^{-1} E_{ck} \tag{36c}$$

and $\bar{r}(kT) = r(t_v + \tau) = r\left[kT + (v+\sigma)T\right]$. The resulting hybrid control system has the configuration as shown in **Figure 4**. It is noted that for $\tau = 0$, *i.e.* in the delay-free case, (35) agrees with the prediction-based digital control law (25c) as $D_{dk} = 0$. Therefore, the prediction-based digital redesign can be taken as a special case of proposed delay-compensating digital redesign.

4. Iterative Procedure for Anti-windup Control

Consider a general nonlinear plant

$$\dot{x}_c(t) = f\left(x_c(t)\right) + G\left(x_c(t)\right) u_c(t) \tag{37a}$$

$$y_c(t) = C x_c(t) \tag{37b}$$

where the symbols are defined as in (14) and (18b), $u_c(t) \in \Re^m$ is the true input vector whose i-th entry has the constraints

$$u_c^i(t) = \begin{cases} U_{\max}^i & \text{if } u_{c,ideal}^i(t) > U_{\max}^i \\ u_{c,ideal}^i(t) & \text{if } U_{\min}^i \le u_{c,ideal}^i(t) \le U_{\max}^i \\ U_{\min}^i & \text{if } u_{c,ideal}^i(t) < U_{\min}^i \end{cases} \tag{38}$$

for $i = 1, 2, \cdots, m$, in which $u_{c,ideal}^i(t) \in \Re$ is the ideal i-th input and $U_{\max}^i, U_{\min}^i \in \Re$ are the top and bottom limits for the i-th input, respectively. For the purpose of simplicity, let $U_{\max}^i = -U_{\min}^i > 0$ in the following reasoning. Through the optimal linearization in Section 2, the optimal local linear model of the nonlinear plant (37) at the k-th sampling instant is obtained as

$$\dot{x}_c(t) = A_k x_c(t) + B_k u_c(t) \tag{39a}$$

$$y_c(t) = C x_c(t) \tag{39b}$$

where (A_k, B_k) are given by (16) and (17), respectively. Should no input saturation occur, *i.e.* $\left|u_{c,ideal}^i(t)\right| \le U_{\max}^i$ for $i = 1, 2, \cdots, m$, the state equation (39a) becomes $\dot{x}_c(t) = A_k x_c(t) + B_k u_{c,ideal}(t)$ as $u_c(t) = u_{c,ideal}(t)$.

Whenever input saturation happens, say, the i-th ideal input $u_{c,ideal}^i(t)$ is out of limits, the state Equation (39a) becomes

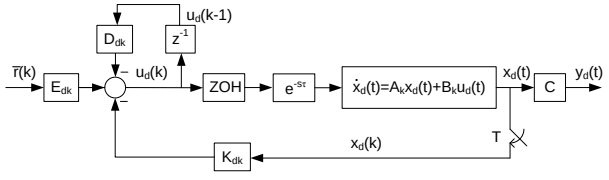

Figure 4. Proposed control scheme for input delay compensation.

$$\dot{x}_c(t) = A_k x_c(t) + B_k \begin{pmatrix} u^1_{c,ideal}(t) \\ u^2_{c,ideal}(t) \\ \vdots \\ U^i_{\max} sign\left(u^i_{c,ideal}(t)\right) \\ \vdots \\ u^m_{c,ideal}(t) \end{pmatrix} \quad (40)$$

which is apparently non-smooth due to the scalar sign function. Substituting approximated scalar sign function (9) for $sign\left(u^i_{c,ideal}(t)\right)$ yields an approximated equation as

$$\dot{x}_c(t) \approx A_k x_c(t) + B_k \begin{pmatrix} \cdots \\ U^i_{\max} sign_j\left(u^i_{c,ideal}(t)\right) \\ \cdots \end{pmatrix} \quad (41)$$

Equation (41) is still nonlinear due to $sign_j\left(u^i_{c,ideal}(t)\right)$ which can be further linearized by *Remark* 2 as

$$sign_j\left(u^i_{c,ideal}(t)\right) \approx \left(\frac{sign_j\left(u^i_{c,ideal}(kT)\right)}{u^i_{c,ideal}(kT)}\right) u^i_{c,ideal}(t)$$

where $u^i_{c,ideal}(kT)$ is the *k*-th operating point of $u^i_{c,ideal}(t)$. In this way, the non-smooth saturation Equation (41) is fully linearized as

$$\begin{aligned} \dot{x}_c(t) &\approx A_k x_c(t) + B_k \begin{pmatrix} u^1_{c,ideal}(t) \\ u^2_{c,ideal}(t) \\ \vdots \\ \bar{\kappa}_{k,i} u^i_{c,ideal}(t) \\ \vdots \\ u^m_{c,ideal}(t) \end{pmatrix} \\ &= A_k x_c(t) + B_k \bar{\kappa}_k u_{c,ideal}(t) = A_k x_c(t) + \bar{B}_k u_{c,ideal}(t) \end{aligned} \quad (42)$$

where

$$\bar{\kappa}_{k,i} = U^i_{\max}\left(\frac{sign_j\left(u^i_{c,ideal}(kT)\right)}{u^i_{c,ideal}(kT)}\right),$$

$$\bar{\kappa}_k = \mathrm{diag}\left\{\underbrace{1,1,\cdots,\bar{\kappa}_{k,i},\cdots,1}_{m}\right\}$$

and $\bar{B}_k = B_k \bar{\kappa}_k$. $\bar{\kappa}_k$ is called input scaling factor.

To prevent the *i*-th input from saturation at $t = kT$, the input scaling factor $\bar{\kappa}_k$ should be tuned such that $\left|\bar{\kappa}_{k,i} u^i_{c,ideal}(t)\big|_{t=kT}\right| = \left|\bar{\kappa}_{k,i} u^i_{c,ideal}(kT)\right| \le U^i_{\max}$, that is

$$\begin{aligned} &\left| U^i_{\max}\left(\frac{sign_j\left(u^i_{c,ideal}(kT)\right)}{u^i_{c,ideal}(kT)}\right) u^i_{c,ideal}(kT)\right| . \\ &= \left|U^i_{\max} sign_j\left(u^i_{c,ideal}(kT)\right)\right| \le U^i_{\max} \end{aligned}$$

As mentioned in *Remark* 1, $\left|sign_j(\sigma)\right| \le 1$ for *j* is even, so the approximation order *j* is always an even number in the proposed anti-windup design.

From the linear state Equation (42), the input matrix $\bar{B}_k$ is required for designing the ideal control input $u_{c,ideal}(t)$, while the input scaling factor $\bar{\kappa}_k$, which determines $\bar{B}_k$, involves the ideal control input $u_{c,ideal}(t)$ at $t=kT$ which has not been designed yet. To break this deadlock, a pre-designed control input is used to estimate $\bar{B}_k$ which is then utilized to design the true control input. For a sampled-data control system, a pre-designed digital control input can be used for this purpose. As a result, the linear state Equation (42) is modified to

$$\begin{aligned} \dot{x}_c(t) &\approx A_k x_c(t) + B_k \hat{\kappa}_k u_{c,ideal}(t) \\ &= A_k x_c(t) + \hat{B}_k u_{c,ideal}(t) \end{aligned} \quad (43)$$

where the estimated input matrix $\hat{B}_k = B_k \hat{\kappa}_k$, the estimated input scaling factor $\hat{\kappa}_k = \mathrm{diag}\left\{\underbrace{1,1,\cdots,\hat{\kappa}_{k,i},\cdots,1}_{m}\right\}$ with

$$\begin{aligned} \hat{\kappa}_{k,i} &= U^i_{\max} \frac{sign_j\left(u^i_{d,ideal}(kT)\right)}{u^i_{d,ideal}(kT)} \\ &= \left(\frac{U^i_{\max}}{u^i_{d,ideal}(kT)}\right) \frac{\left(1+u^i_{d,ideal}(kT)\right)^j - \left(1-u^i_{d,ideal}(kT)\right)^j}{\left(1+u^i_{d,ideal}(kT)\right)^j + \left(1-u^i_{d,ideal}(kT)\right)^j} \end{aligned} \quad (44)$$

for *j* is even. $u^i_{d,ideal}(kT)$ is the pre-designed digital control input which can be the digitally redesigned control input for the *i*-th component of $u_{c,ideal}(t)$ at $t = kT$ from the prediction-based digital redesign (25c) or the proposed delay-compensating digital redesign (35). With arbitrary input elements saturated, the state Equation (43) is generalized as

$$\begin{aligned} \dot{x}_c(t) &\approx A_k x_c(t) + B_k \hat{\kappa}_k u_{c,ideal}(t) \\ &= A_k x_c(t) + \hat{B}_k u_{c,ideal}(t) \end{aligned} \quad (45)$$

with $\hat{\kappa}_k = \mathrm{diag}\left\{\hat{\kappa}_{k,i}\right\}$ for $i = 1,2,\cdots,m$, where $\hat{\kappa}_{k,i} = 1$ or is given by (44) depending on whether the corresponding ideal input violates the constraints or not.

The general saturated state Equation (45) and the output Equation (39b) form a saturated system with modified system matrices $\left(A_k, \hat{B}_k, C\right)$. Applying LQR (21-23) to it yields that with weighting matrices (*Q*, *R*), the optimal control law is determined by solving the Riccati equation

$$A_k^{\mathrm{T}} \hat{P}_k + \hat{P}_k A_k - \hat{P}_k \hat{B}_k R^{-1} \hat{B}_k^{\mathrm{T}} \hat{P}_k + C^{\mathrm{T}} Q C = 0 \quad (46)$$

which can be rewritten as

$$A_k^{\mathrm{T}} \hat{P}_k + \hat{P}_k A_k - \hat{P}_k B_k \hat{R}^{-1} B_k^{\mathrm{T}} \hat{P}_k + C^{\mathrm{T}} Q C = 0 \quad (47)$$

where $\hat{R} = \hat{\kappa}_k^{-1} R \hat{\kappa}_k^{-1}$. The resulting optimal control law is

$$u_{c,ideal}(t) = -\hat{K}_{ck} x_c(t) + \hat{E}_{ck} r(t) \qquad (48)$$

where the feedback gain

$\hat{K}_{ck} = R^{-1}\hat{B}_k^{\mathrm{T}}\hat{P}_k = \hat{\kappa}_k^{-1}\hat{R}^{-1}B_k^{\mathrm{T}}\hat{P}_k = \hat{\kappa}_k^{-1}\bar{K}_{ck}$

with $\bar{K}_{ck} = \hat{R}^{-1}B_k^{\mathrm{T}}\hat{P}_k$, and the forward gain

$$\hat{E}_{ck} = -R^{-1}\hat{B}_k^{\mathrm{T}}\left[\left(A_k - \hat{B}_k\hat{K}_{ck}\right)^{-1}\right]^{\mathrm{T}} C^{\mathrm{T}}Q$$

$$= -\hat{\kappa}_k^{-1}\hat{R}^{-1}B_k^{\mathrm{T}}\left[\left(A_k - B_k\bar{K}_{ck}\right)^{-1}\right]^{\mathrm{T}} C^{\mathrm{T}}Q = \hat{\kappa}_k^{-1}\bar{E}_{ck}$$

with $\bar{E}_{ck} = -\hat{R}^{-1}B_k^{\mathrm{T}}\left[\left(A_k - B_k\bar{K}_{ck}\right)^{-1}\right]^{\mathrm{T}} C^{\mathrm{T}}Q$.

On the other hand, applying LQR to the original system (A_k, B_k, C) in (39) with the modified weighting pair $(Q, \hat{R})$ yields the optimal control law

$$u_c(t) = -\bar{K}_{ck} x_c(t) + \bar{E}_{ck} r(t) \qquad (49)$$

where the feedback gain $\bar{K}_{ck}$ and the forward gain $\bar{E}_{ck}$ are shown above. The corresponding Riccati equation is the same as (47).

It can be observed by comparing the above two LQR designs that the problem of finding the optimal control law for the saturated system (45) with the weighting matrices (Q, R) can be reformulated as the same problem for the original system (39) using the same performance index (19), but with the new weighting matrices $(Q, \hat{R})$ where $\hat{R} = \hat{\kappa}_k^{-1} R \hat{\kappa}_k^{-1}$. Generally, both weighting matrices are selected to be positive definite diagonal matrices. So when the input scaling factor's i-th diagonal element $\hat{\kappa}_{k,i} < 1$, the corresponding i-th diagonal elements of R and $\hat{R}$ have the relationship of $\hat{R}_i = \hat{\kappa}_{k,i}^{-1} R_i \hat{\kappa}_{k,i}^{-1} > R_i$. As the matrix Q is kept the same in the performance index, the resulting control law $u_{c,ideal}(t)$ with $(Q, \hat{R})$ will have a smaller i-th element than the counterpart with (Q, R). Accordingly, the corresponding i-th element of digitally redesigned control input $u_{d,ideal}(t)$ would be smaller as well, thus possibly avoiding input saturation. It is noted that although $\hat{R}_i$ is $\hat{\kappa}_{k,i}^{-2}$ times greater than R_i, the newly resulting digital input $u_{d,ideal}^i(t)$ is not necessarily $\hat{\kappa}_{k,i}^{-2}$ times smaller than the original one and may be still out of input limits after a single update. Therefore, it might be necessary to recursively update on $\hat{R}_i$ until the input lies within the saturation limits. **Figure 5** summarizes the general steps of proposed anti-windup digital controller design for analog nonlinear system with input constraints. The digital redesign adopted is the proposed delay-compensating technique, so besides the anti-windup functionality, the proposed digital controller can also survive in a time-delayed environment.

Remark 3: The approximation order j in the approximated scalar sign function can be tuned to achieve certain tradeoff between the control performance and the recursion efficiency. As shown in **Figure 1**, a smaller approximation order j leads to a faster decaying approximated scalar sign function, which results in a smaller $\hat{\kappa}_{k,i}$. This can be regarded as an 'aggressive' update scheme with the advantage that a smaller number of iterations are needed for suppressing the input to within the limits. But the disadvantage is that the input could be suppressed too much below the limit, which may bring a fairly slow system response.

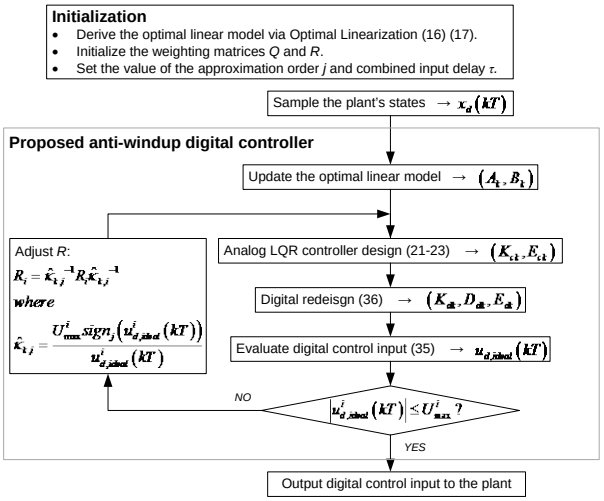

Figure 5. Anti-windup plus delay-compensating digital controller.

5. Simulation Results

As a typical nonlinear system, the rotary inverted pendulum system depicted in **Figure 6** presents many challenging topics for investigation, like coupling, underactuation, instability, multivariable, time-sensitivity etc. The pendulum control can be simply categorized into swing-up (the motor drives the L-shaped arm to swing the pendulum up to around the upright position) and stabilization (the motor drives the arm to stabilize the pendulum at the upright position). Nonlinear control methods are usually proposed for swing-up control while LQR is commonly used for stabilization control. The failure to apply LQR on swing-up control results from the deficiency of traditional linearization method which only works around the equilibrium points while the pendulum is running in off-equilibrium region in swing-up process. In the proposed anti-windup design, the optimal linearization approach is utilized to obtain the local linear model at any operating point, and then LQR is applied to produce a state-feedback controller optimal for each operating point. Therefore, the proposed design can be applied throughout both swing-up and stabilization processes, avoiding the trouble of switching controllers in conventional methods.

The dynamics between the arm angle θ, the pendulum angle α and the motor voltage V_m is derived using La-

grangian equations as

$$\ddot{\theta} = \left(c_{11}\sin\alpha\cos^2\alpha\dot{\theta}^2 + c_{12}\sin\alpha\dot{\alpha}^2 + c_{13}\sin\alpha\cos\alpha\dot{\theta}\dot{\alpha} + c_{14}\sin\alpha\cos\alpha + c_{15}\dot{\theta} + c_{16}V_m\right)\Big/\left(d_1 + d_2\sin^2\alpha\right) \tag{50a}$$

$$\ddot{\alpha} = \left(c_{21}\sin\alpha\cos\alpha\dot{\theta}^2 + c_{22}\sin^3\alpha\cos\alpha\dot{\theta}^2 + c_{23}\sin\alpha\cos\alpha\dot{\alpha}^2 + c_{24}\sin\alpha\cos^2\alpha\dot{\theta}\dot{\alpha} + c_{25}\sin^3\alpha + c_{26}\sin\alpha + c_{27}\cos\alpha\dot{\theta} + c_{28}\cos\alpha V_m\right)\Big/\left(d_1 + d_2\sin^2\alpha\right) \tag{50b}$$

where

$$c_{11} = -M_p l_p J_p r\,,\quad c_{12} = M_p l_p J_p r\,,\quad c_{13} = -2J_p^2\,,$$
$$c_{14} = -M_p^2 l_p^2 r g\,,\quad c_{15} = -J_p K_t K_m / R_m\,,\quad c_{16} = J_p K_t / R_m\,,$$
$$c_{21} = \left(J_{eq} + M_p r^2\right) J_p\,,\quad c_{22} = J_p^2\,,\quad c_{23} = -M_p^2 l_p^2 r^2\,,$$
$$c_{24} = 2M_p l_p J_p r\,,\quad c_{25} = M_p l_p J_p g\,,$$
$$c_{26} = \left(J_{eq} + M_p r^2\right) M_p l_p g\,,\quad c_{27} = M_p l_p r K_t K_m / R_m\,,$$
$$c_{28} = -M_p l_p r K_t / R_m\,,\quad d_1 = J_{eq} J_p + M_p r^2 J_p - M_p^2 l_p^2 r^2\,,$$
$$d_2 = J_p^2 + M_p^2 l_p^2 r^2\,.$$

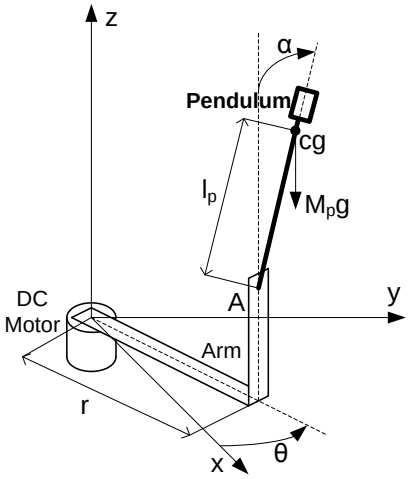

Figure 6. Single rotary inverted pendulum.

The parameters have physical meanings defined in **Table 1** as well as their values used in the following simulations. Apparently, (50) is highly nonlinear and coupled expressions.

For space-saving purpose, the derivation of optimal local linear model of (50) is skipped, and only salient simulation results and necessary explanations are presented here. The proposed anti-windup methodology in **Figure 5** was implemented in simulations with the initial pendulum angle of 179° (almost the downward position), the initial weighting matrices Q = diag{50, 0, 1, 0} and R = 1, and the digital control period T = 0.01 s. **Figure 7** compares the simulated control performances of proposed method under no input limit and the limits ±30 V with different approximation order j. The corresponding control inputs are shown in **Figure 8**. Obviously, the freely redesigned digital control voltage in **Figure 8** is out of the limits ±30 V over multiple control periods; using the proposed anti-windup method, whatever the value of j is, the control voltage is successfully suppressed to within the specified limits ±30 V. Another apparent fact is that over the first few control periods, the control voltage for j = 16 is suppressed more than the one for j = 26, which results in a little slower control performance in **Figure 7**. This echoes the claims by *Remark* 3. No time delay is introduced in the control loop in this case, so the proposed delay-compensating digital control law (35) converges to the prediction-based digital control law (25c) and the parameter v is set to 1.

Next, an input time delay is introduced between the pendulum's motor and the digital controller to represent

Table 1. Single rotary inverted pendulum nomenclature.

Symbol	Description	Value	Unit
M_p	Mass of the pendulum assembly (weight and link combined).	0.027	kg
l_p	Length of pendulum center of gravity from pivot.	0.156	m
r	Length of arm pivot to pendulum pivot.	0.0826	m
J_{eq}	Equivalent moment of inertia about motor shaft pivot axis.	1.23e−4	kg·m^2
J_p	Pendulum moment of inertia about its pivot axis.	7.3e−4	kg·m^2
R_m	Motor armature resistance.	3.3	Ω
K_t	Motor torque constant.	0.02797	N·m
K_m	Motor back-electromotive force constant.	0.02797	V/(rad/s)
g	Gravitational acceleration constant.	9.81	m/s^2

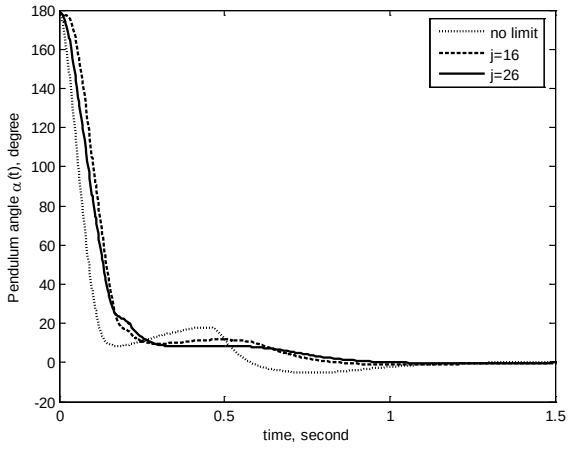

Figure 7. Control performance of proposed design in the delay-free case.

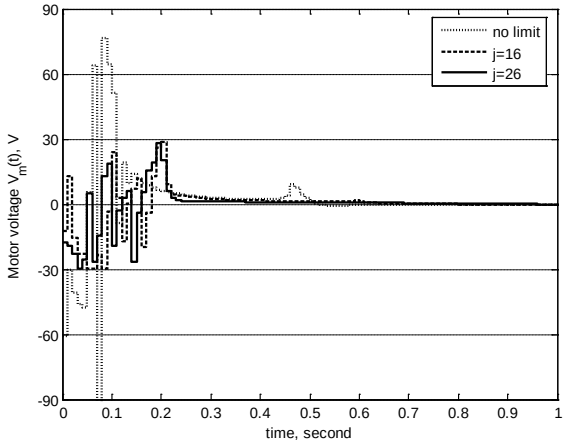

Figure 8. Control inputs of proposed design in the delay-free case.

the potential time delays in the real-world control loop. In order to demonstrate the delay-compensating capability, a reasonably long time delay τ = 0.02 s is used. The control period T is accordingly extended to 0.02 s as the proposed design assumes a control period no shorter than the delay duration. Other parameters and initial conditions are the same as the delay-free case. Simulation results showed that the controller from the prediction-based digital redesign cannot succeed any more, exhibiting an unstable behavior. In contrast, the proposed anti-windup plus delay-compensating controller can still survive with performances shown in **Figure 9**. **Figure 10** depicts the evolutions of control inputs: the motor voltages in constrained cases are successfully suppressed to within the desired range. Hence, the efficacy of proposed design is well demonstrated.

6. Conclusions

This paper describes the design and application of an optimal anti-windup digital controller for analog nonlinear plants subject to input constraints. As a new anti-windup technique for sampled-data control systems, the proposed method has the following contributions: 1) the approximated scalar sign function is utilized to model non-smooth input saturations, which presents a new effective solution to sign-function constrained non-smooth problems; 2) through the optimal linearization, a general approach is developed for handling nonlinear systems with linear control theories in a broader region instead of conventionally being limited to around equilibriums; 3) aside from the anti-windup functionality, the proposed digital controller is capable of compensating time delays in the control loop, which would help guarantee its designed performance in real world implementations.

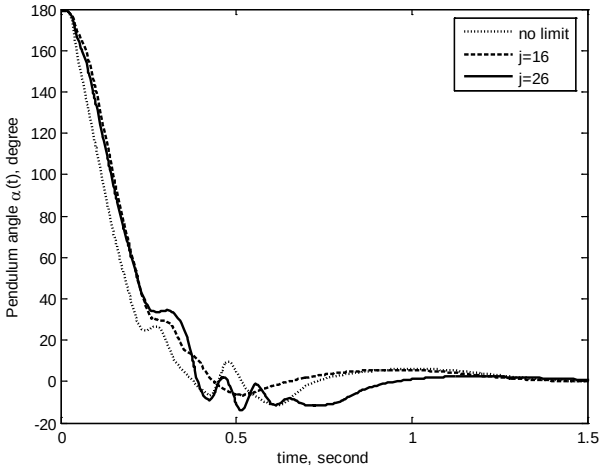

Figure 9. Control performance of proposed design in the delayed case.

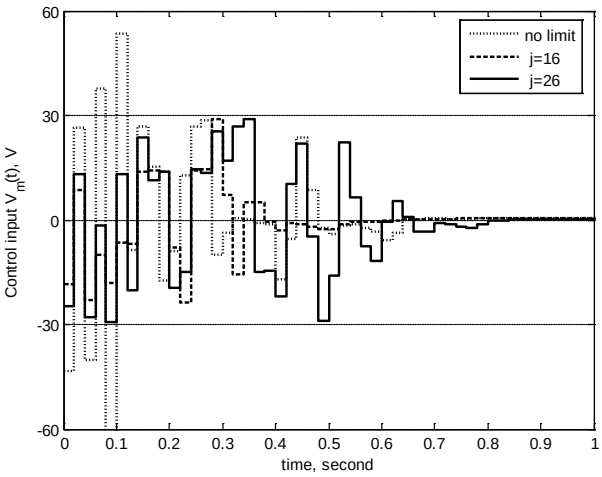

Figure 10. Control inputs of proposed design in the delayed case.

Funding

Research supported by NSF award #1238859, and De-

partment of Education, HBGI Grant.

REFERENCES

[1] M. V. Kothare, P. J. Campo, M. Morari and C. N. Nett, "A Unified Framework for the Study of Antiwindup Designs," *Automatica*, Vol. 30, No. 12, 1994, pp. 1869-1883. http://dx.doi.org/10.1016/0005-1098(94)90048-5

[2] C. Edwards and I. Postlethwaite, "Anti-Windup, Bumpless-Transfer Schemes," *Automatica*, Vol. 34, No. 2, 1998, pp. 199-210. http://dx.doi.org/10.1016/S0005-1098(97)00165-9

[3] P. Westen and I. Postlethwaite, "Linear Conditioning for Systems Containing Saturating Actuators," *Automatica*, Vol. 36, No. 9, 2000, pp. 1347-1354. http://dx.doi.org/10.1016/S0005-1098(00)00044-3

[4] Y. S. Chen, J. S. H. Tsai, L. S. Shieh and F. C. Kung, "New Conditioning Dual-Rate Digital-Redesign Scheme for Continuous-Time Systems with Saturating Actuators," *IEEE Transactions on Circuits and Systems I*: *Fundamental Theory and Applications*, Vol. 49, No. 12, 2002, pp. 1860-1870. http://dx.doi.org/10.1109/TCSI.2002.805731

[5] V. R. Marcopoli and S. M. Phillips, "Analysis and Synthesis Tools for a Class of Actuator-Limited Multivariable Control Systems: A Linear Matrix Inequality Approach," *International Journal of Robust and Nonlinear Control*, Vol. 6, No. 9-10, 1996, pp. 1045-1063. http://dx.doi.org/10.1002/(SICI)1099-1239(199611)6:9/10<1045::AID-RNC268>3.0.CO;2-S

[6] E. F. Mulder, M. V. Kothare and M. Morari, "Multivariable Anti-Windup Controller Synthesis Using Linear Matrix Inequalities," *Automatica*, Vol. 37, No. 9, 2001, pp. 1407-1416. http://dx.doi.org/10.1016/S0005-1098(01)00075-9

[7] G. Grimm, J. Hatfield, I. Postlethwaite, A. R. Teel, M. C. Turner and I. Zaccarian, "Anti-Windup for Stable Linear Systems with Input Saturations: A LMI Based Synthesis," *IEEE Transactions on Automatic Control*, Vol. 48, No. 9, 2003, pp. 1509-1525. http://dx.doi.org/10.1109/TAC.2003.816965

[8] J. R. Calvet and Y. Arkun, "Feedforward and Feedback Linearization of Nonlinear Systems and Its Implementation Using IMC," *Industrial & Engineering Chemistry Research*, Vol. 27, No. 10, 1988, pp. 1822-1831. http://dx.doi.org/10.1021/ie00082a015

[9] L. Del Re, J. Chapuis and V. Nevistic, "Predictive Control with Embedded Feedback Linearization for Bilinear Plants with Input Constraints," *Proceedings of the* 43rd *IEEE Conference on Decision and Control*, San Antonio, 15-17 December 1993, pp. 2984-2989.

[10] T. A. Kendi and F. J. Doyle, "An Anti-Windup Scheme for Multivariable Nonlinear System," *Journal of Process Control*, Vol. 7, No. 5, 1997, pp. 329-343. http://dx.doi.org/10.1016/S0959-1524(97)00011-5

[11] Q. Hu and G. O. Rangaiah, "Anti-Windup Schemes for Uncertain Nonlinear Systems," *IEE Proceedings of Control Theory and Applications*, Vol. 147, No. 3, 2000, pp. 321-329. http://dx.doi.org/10.1049/ip-cta:20000136

[12] R. Bouc, "Forced Vibration of Mechanical Systems with hysteresis," *Proceedings of* 4th *Conference Nonlinear Oscillation*, Prague, 5-9 September 1967, p. 315.

[13] Y. K. Wen, "Method for Random Vibration of Hysteretic Systems," *Journal of Engineering Mechanics Division*, 1976, pp. 249-263.

[14] B. Jacobson, "The Stribeck Memorial Lecture," *Tribology International*, Vol. 36, 2003, pp. 781-789.

[15] L. S. Shieh, Y. T. Tsay and R. Yates, "Some Properties of Matrix Sign Functions Derived from Continued Fractions," *IEEE Proceedings of Control Theory and Applications, Part D*, Vol. 130, 1983, pp. 111-118.

[16] L. S. Shieh, Y. T. Tsay and C. T. Wang, "Matrix Sector Functions and Their Applications to Systems Theory," *IEEE Proceedings of Control Theory and Applications, Part D*, Vol. 131, 1984, pp. 171-181.

[17] M. C. M. Teixeira and S. H. Zak, "Stabilizing Controller Design for Uncertain Nonlinear Systems Using Fuzzy Models," *IEEE Transaction on Fuzzy Systems*, Vol. 7, No. 2, 1999, pp. 133-142. http://dx.doi.org/10.1109/91.755395

[18] J. D. Roberts, "Linear Model Reduction and Solution of the Algebraic Riccati Equations by Use of the Sign Function," *International Journal of Control*, Vol. 32, No. 4, 1980, pp. 677-687. http://dx.doi.org/10.1080/00207178008922881

[19] F. Esfandiari and H. K. Khalil, "Output Feedback Stabilization of Fully Linearizable Systems," *International Journal of Control*, Vol. 56, No. 5, 1992, pp. 1007-1037. http://dx.doi.org/10.1080/00207179208934355

[20] S. M. Guo, L. S. Shieh, G. Chen and C. F. Lin, "Effective Chaotic Orbit Tracker: A Prediction-Based Digital Redesign Approach," *IEEE Transaction on Circuits and Systems*, Vol. 47, 2000, pp. 1557-1570.

[21] F. L. Lewis, "Optimal Control," Wiley, New York, 1986.

[22] K. Ogata, "Discrete-Time Control Systems," Prentice-Hall, Englewood Cliffs, 1987.

[23] J. S. H. Tsai, C. M. Chen and L. S. Shieh, "Digital Redesign of the Cascaded Continuous-Time Controller: Time-Domain Approach," *Control Theory Advanced Techniques*, Vol. 17, 1991, pp. 643-661.

[24] L. S. Shieh, W. M. Wang and M. K. A. Panicker, "Design of PAM and PWM Digital Controllers for Cascaded Analog Systems," *ISA Transaction*, Vol. 37, No. 3, 1998, pp. 201-213. http://dx.doi.org/10.1016/S0019-0578(98)00026-3

[25] L. S. Shieh, J. L. Zhang and N. P. Coleman, "Optimal Digital Redesign of Continuous-Time Controllers," *Computers & Mathematics with Applications*, Vol. 22, No. 1, 1991, pp. 25-35. http://dx.doi.org/10.1016/0898-1221(91)90022-V

[26] H. Wang, L. S. Shieh, Y. Zhang and J. S. Tsai, "Minimal Realization of the Transfer Function Matrix with Multiple Time Delays," *IET Control Theory and Application*, Vol. 1, No. 5, 2007, pp. 1294-1301. http://dx.doi.org/10.1049/iet-cta:20060281